

Supplementary materials

Matching experimental chemical composition configuration and theoretical model in $\text{Nd}_2\text{Fe}_{14}\text{B}/\alpha\text{-Fe}$ nanocomposites to improve coercivity

Yuqing Li, Jinjin Wang, Manying Liu, Xuerui Xu, Mengying Bian*, Weiqiang Liu, Dongtao Zhang, Hongguo Zhang, Ming Yue*

College of Materials Science and Engineering, Key Laboratory of Advanced Functional Materials, Ministry of Education of China, Beijing University of Technology, Beijing, 100124, China

*Address correspondence to E-mail: bianmy@bjut.edu.cn (Mengyin Bian), yueming@bjut.edu.cn (Ming Yue)

SM-I: The amorphous $\text{Nd}_2\text{Fe}_{14}\text{B}/\alpha\text{-Fe}$ ribbons

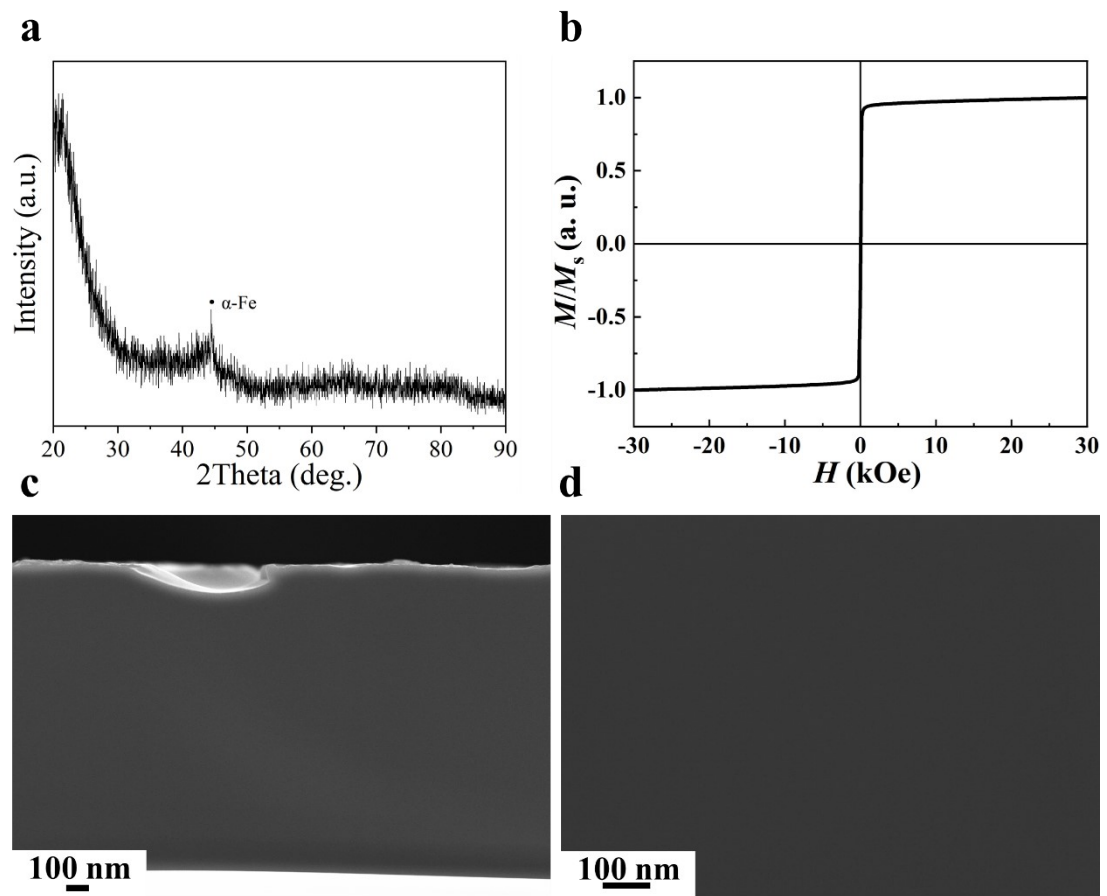


Fig. S1 The amorphous $\text{Nd}_2\text{Fe}_{14}\text{B}/\alpha\text{-Fe}$ ribbons. a: XRD pattern; b: hysteresis loops; c and d: SEM fracture morphology.

SM-II: Magnetic properties of the annealed amorphous ribbons

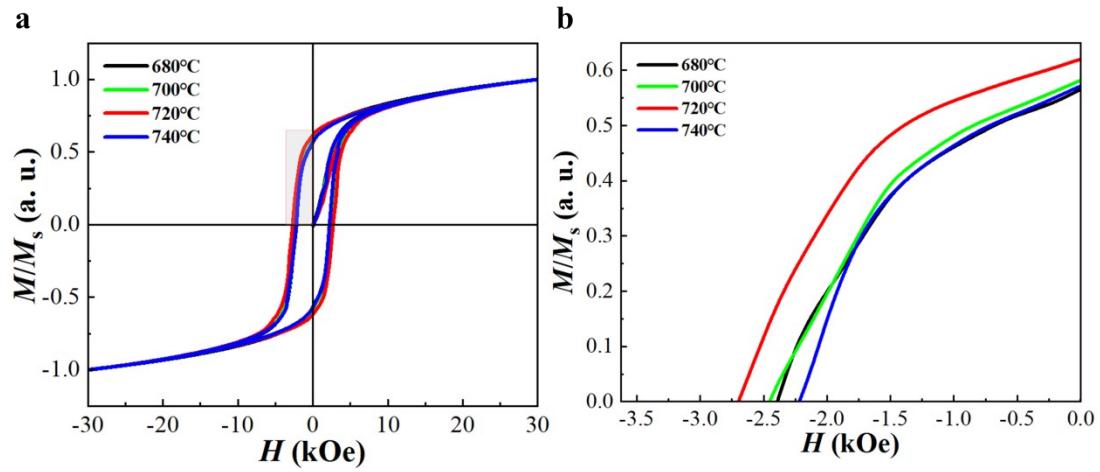


Fig. S2 Hysteresis loops (a) and demagnetization curves (b) of amorphous $\text{Nd}_2\text{Fe}_{14}\text{B}/\alpha\text{-Fe}$ ribbons annealed at different temperatures.

SM-III: Two typical ideal soft-hard composite models

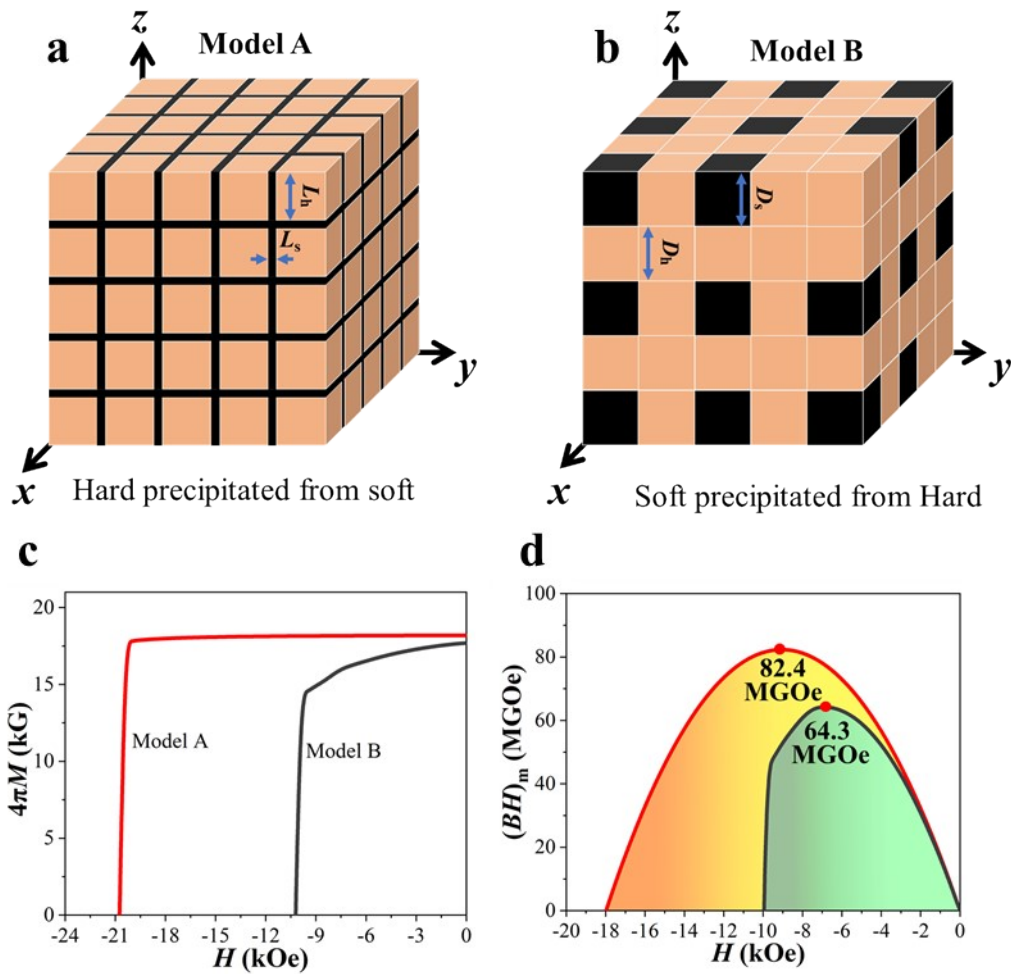


Fig. S3 Two typical soft hard composite models; a and b showing the diagrams of Model A and Model B, the hard phase precipitated on the soft phase matrix and the soft phase precipitated on the hard phase matrix respectively; c and d are demagnetization curves and magnetic energy product curves obtained from the two models, respectively.

SM-IV: SEM graphs of the Tips for 3DAP

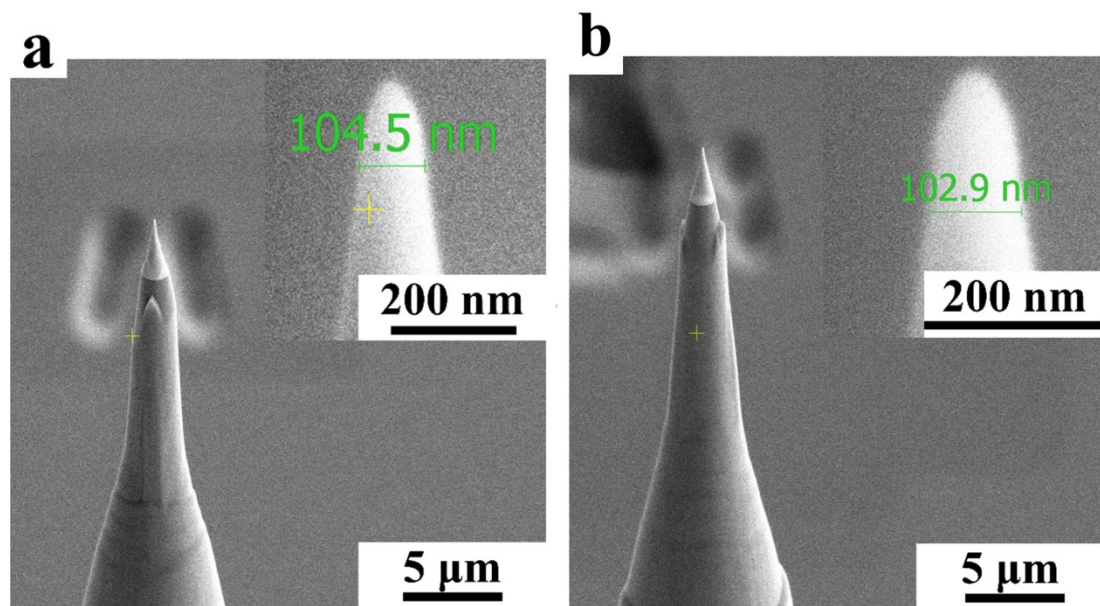


Fig. S4 The SEM graphs of the tips of Sample A (a) and Sample B (b).

SM-V: Video 1 for 3D structure of sample A.

SM-VI: Video 2 for 3D structure of sample B.